Biophysical Journal
Article

Biophysical Society

Different membrane order measurement techniques are not mutually consistent

Ankur Gupta,[1] Mamata Kallianpur,[1] Debsankar Saha Roy,[1] Oskar Engberg,[2] Hirak Chakrabarty,[3] Daniel Huster,[1,2,*] and Sudipta Maiti[1,*]

[1]Tata Institute of Fundamental Research, Colaba, Mumbai, India; [2]Institute of Medical Physics and Biophysics, University of Leipzig, Leipzig, Germany; and [3]School of Chemistry, Sambalpur University, Burla, Odisha, India

ABSTRACT "Membrane order" is a term commonly used to describe the elastic and mechanical properties of the lipid bilayer, though its exact meaning is somewhat context- and method dependent. These mechanical properties of the membrane control many cellular functions and are measured using various biophysical techniques. Here, we ask if the results obtained from various techniques are mutually consistent. Such consistency cannot be assumed a priori because these techniques probe different spatial locations and different spatial and temporal scales. We evaluate the change of membrane order induced by serotonin using nine different techniques in lipid bilayers of three different compositions. Serotonin is an important neurotransmitter present at 100s of mM concentrations in neurotransmitter vesicles, and therefore its interaction with the lipid bilayer is biologically relevant. Our measurement tools include fluorescence of lipophilic dyes (Nile Red, Laurdan, TMA-DPH, DPH), whose properties are a function of membrane order; atomic force spectroscopy, which provides a measure of the force required to indent the lipid bilayer; ^{2}H solid-state NMR spectroscopy, which measures the molecular order of the lipid acyl chain segments; fluorescence correlation spectroscopy, which provides a measure of the diffusivity of the probe in the membrane; and Raman spectroscopy, where spectral intensity ratios are affected by acyl chain order. We find that different measures often do not correlate with each other and sometimes even yield conflicting results. We conclude that no probe provides a general measure of membrane order and that any inference based on the change of membrane order measured by a particular probe may be unreliable.

SIGNIFICANCE This work highlights the need for understanding the response of different techniques used in investigating lipid membrane order. Inference about the increase (or decrease) of membrane order measured by any particular technique is typically assumed to be valid irrespective of the biophysical tool used. However, these techniques measure somewhat different properties related to membrane order, and there is no a priori reason for them to be in agreement. Our systematic study involving nine different methods shows that the outputs of these measurements do not universally correlate with each other. Moreover, they frequently show opposite directions for the change of membrane order under a specific perturbation that is biologically relevant. Thus, interpretation of biological consequences by measuring the membrane order using a single probe may be unreliable.

INTRODUCTION

The term "membrane order" is generally used to describe the mechanical properties of lipid bilayer membranes. Mechanical properties play a crucial role in various key cellular functions such as structure and functions of membrane proteins (1), signal transduction (2–5), receptor translocation (6), and mitochondria metabolism (7). Studies showed that alteration in membrane order causes cellular dysfunction (8–11) and acts as a reporter for identifying and targeting many diseases (12–14). Though membrane order typically relates to lipid packing and dynamics in the membrane, its definition is context dependent. A large range of biophysical techniques has been developed to measure this quantity. Any inference drawn from a measurement performed with a particular technique will be robust only when it is known that it correlates well with other techniques. In this work, we have measured membrane order using multiple techniques to evaluate the correlation among these measurements.

Environment- and polarity-sensitive fluorescent dyes are the most commonly used probes of membrane order because

Submitted June 7, 2022, and accepted for publication August 19, 2022.

*Correspondence: daniel.huster@medizin.uni-leipzig.de or maiti@tifr.res.in

Editor: Michael F. Brown.

https://doi.org/10.1016/j.bpj.2022.08.029

of their compatibility with live-cell measurements (15–18). For example, the maximum emission peak in the fluorescence spectrum of the dye Nile Red shifts to a lower wavelength if the environment becomes less polar. The lower polarity inside the membrane is a result of the tighter packing of hydrophobic lipid tails, which indicates an increase in membrane order (19). Therefore, a ratio of the Nile Red emission in the green region (569–604 nm) to that in the red region (624–659 nm), the so-called G/R ratio, provides a measure of membrane order. The other commonly used membrane polarity-sensitive dye is Laurdan (20), which has a red-shifted fluorescence emission (peak at ~490 nm) in disordered membranes and a blue-shifted fluorescence in ordered membranes (peak at ~440 nm). The order of the membrane is quantified by a ratiometric parameter, known as generalized polarization (GP). GP is defined as a normalized ratio of fluorescence intensities $(I_{440} - I_{490})/(I_{440} + I_{490})$ (20). It has been shown that the GP of Laurdan is linearly dependent on membrane tension in model membranes (21). Other fluorescent probes such as Prodan, DPH, TMA-DPH, pyrene and its derivatives, N-(7-Nitrobenz-2-oxa-1,3-diazol-4-yl), and DiI are also used to determine membrane order (22). Eight different polarity-sensitive dyes have been shown (23) to have a reasonably good qualitative correlation for membrane order measurement, though they have different sensitivities, likely due to their local position and orientation (22). However, Laurdan and Patman fluorescence spectra (24) do not seem to correlate in their sensitivity to membrane cholesterol molar fraction.

There are other techniques to probe the order of the membrane, such as atomic force microscopy (AFM), fluorescence correlation spectroscopy (FCS), Raman spectroscopy, and NMR. AFM measures the stiffness of the membrane by measuring the amount of force (known as breakthrough force) required to rupture the bilayer locally by a sharp AFM tip (25,26). In general, higher stiffness (i.e., greater breakthrough force) is correlated with higher ordering of the membrane. FCS measures the translational diffusion coefficients (D_T) of membrane lipids (27). A smaller D_T indicates a more ordered membrane. Z-scan FCS is a special FCS methodology employed to determine the diffusion coefficient of planar-supported bilayers and avoids nontrivial external calibration of the size of the detection volume (28). Raman spectroscopy is also used to measure the order of the membrane. The Raman spectra of the ν(C-H) region of the membrane are sensitive to lipid packing and local lipid dynamics (29,30). Specifically, the ratios of intensities I_{2885}/I_{2850} and I_{2850}/I_{2930} provide the average CH_2 conformational order (or lateral order) and terminal CH_3 rotational order of the membrane. These ratios are related to the order of the membrane. Perhaps the most direct atomic-level measurement of the order of the lipid acyl chains can be obtained from solid-state NMR measurements. Time-averaged orientational fluctuations of the C–^{2}H bond vectors of lipid chains, obtained from residual quadrupolar couplings measurement in ^{2}H NMR, give the orientational (or segmental) order parameter for each C–^{2}H group (31–33). The same information is also available from measurements of the motionally averaged ^{1}H-^{13}C dipolar couplings under magic angle spinning conditions (34,35).

Typically, inferences on membrane order are drawn from studies using a single membrane probe (36–40). A few studies have utilized multiple types of membrane probes to determine the order of the membrane and observed good qualitative correlation between GP and bending rigidity measurements (41), NMR order parameter and GP measurements (42), and GP and AFM breakthrough force (F_X) measurements (26). However, these studies have used only a few probes (two or three) and a single membrane composition. Thus, it is not obvious whether the correlation is universal among a large range of techniques and different types of bilayers.

Here, we have expanded the number of techniques to nine, applying them to lipid bilayers consisting of POPC (1-palmitoyl-2-oleoyl-glycero-3-phosphocholine)/POPG (1-palmitoyl-2-oleoyl-sn-glycero-3-phospho-(1'-rac-glycerol))/cholesterol in the molar ratio of 1/1/1 (PPC111). A subset of these techniques was also applied to several different membrane compositions. The techniques we employed were AFM, NMR, z-scan FCS, Raman, and fluorescence spectroscopy of Nile Red, Laurdan, DPH, and TMA-DPH dyes. Instead of correlating absolute values of the membrane order, we have assessed the change in membrane order induced by a perturbation, arguing that a change in membrane order should correlate more strongly across different probes and techniques. The perturbative agent is serotonin, a neurotransmitter whose interaction with the lipid membrane has been a focus of recent biophysical research (25,43–47). We used the small lipophilic molecule serotonin to induce changes in membrane order. Serotonin and serotonin-like molecules modulate membrane order, as shown by our previous studies (25,46–48). We compared both the magnitude and the direction of change for each of these systems and found that the values and the directions frequently do not correlate between techniques.

MATERIALS AND METHODS

The details of the materials and methods are provided in the supporting material. In brief, supported bilayers (SLBs) are prepared on the freshly cleaved mica substrates by following the vesicle fusion method (49). The different compositions were pure POPG, POPC/POPG/cholesterol at a molar ratio of 1/1/1 (PPC111), and DOPC (1,2-dioleoyl-sn-glycero-3-phosphocholine)/egg sphingomyelin/cholesterol at a molar ratio of 2/2/1/ (DEC221). The AFM force indentation study was performed on the SLBs using a commercial NanoWizard II system. The membrane was ruptured locally by the AFM tip, and the force required to rupture it is quantified as F_X. The fluorescence spectra of Nile Red incubated SLBs were obtained by performing confocal imaging in the lambda stacking mode on the commercial LSM 880. One μM Nile Red was incubated to SLBs for 20 min, and unbound Nile Red was washed thoroughly. The multiphoton imaging of Laurdan incubated SLBs is performed by exciting the Laurdan using a

780 nm pulsed laser source and collecting the emission in two channels—blue (410–440 nm) and green (485–515). These channel images were used to obtain GP of Laurdan in the membrane. The diffusion coefficients of lipids in the SLBs were obtained by performing z-scan FCS. The autocorrelation curves were obtained at different z-intervals (along the bilayer axis) using a home-built AFM-confocal instrument and fitted to obtain diffusion coefficients of lipids in the SLBs. The Raman spectra and corresponding ratios I_{2885}/I_{2850} and I_{2850}/I_{2930} were obtained by recording the Raman spectra of SLBs with a home-built line-confocal Raman microscope. Steady-state anisotropy of DPH and TMA-DPH was measured using Hitachi F-7000 (Japan) spectrofluorometer. Both the fluorophores were excited at 360 nm, and the corresponding emissions were measured at 430 nm. For ^{2}H solid-state NMR, multilamellar vesicles were produced by codissolving lipids and serotonin in organic solvents; after evaporating the solvents and lyophilization, the samples were hydrated and equilibrated by freeze thawing. Order parameter profiles were calculated from the dePaked ^{2}H NMR spectra of the deuterated lipid measured on a Bruker 750 Avance I NMR spectrometer (33).

RESULTS

Serotonin-induced perturbation of PPC111 membranes

AFM force indentation

In our previous studies (25), we have measured the F_X of PPC111 SLBs in the absence and the presence of 5 mM serotonin using the AFM force indentation technique. Fig. 1 *B* (reproduced from Dey et al. (25)) shows the representative histograms of F_X of PPC111 in the absence (black) and the presence (red) of 5 mM serotonin. The histogram shows that the F_X of the PPC111 bilayer decreases by 58% ± 19% (25), suggesting that the PPC111 bilayer becomes more disordered in the presence of 5 mM serotonin.

Spectral imaging of Nile Red

We have performed the spectral imaging of the lipophilic dye Nile Red bound to PPC111 SLB in the absence and the presence of 5 mM serotonin to measure the serotonin-induced change in the Nile Red fluorescence spectra. The serotonin-containing membrane has clearly blue-shifted fluorescence spectra (Fig. 1 *D*, *red*) compared with that without serotonin (Fig. 1 *D*, *black*). We have calculated the G/R ratio to quantify the membrane order by Nile Red. The average G/R ratio in the absence and presence of serotonin is 0.73 ± 0.07 and 1.13 ± 0.03, respectively. Thus, the average G/R increases by 55% ± 12%. This suggests that the PPC111 membrane becomes more ordered after 5 mM serotonin addition.

Spectral imaging of Laurdan

We have performed multiphoton imaging (which effectively accesses the UV excitation wavelengths using near infrared light) of the lipophilic Laurdan dye bound to PPC111 SLB in the absence and the presence of 5 mM serotonin to measure the channel-specific fluorescence intensity and then processed them to obtain GP images. Serotonin was incubated with the bilayer for 45 min. The multiphoton imaging was required, as conventional fluorimeter measurements cannot be performed on the SLBs. The representative GP images of the PPC111 SLB in the absence and presence of 5 mM serotonin are shown in Fig. 1 *H* and *L*, respectively. The average GP value of the PPC111 bilayer in the absence (Fig. 1 *M*, *black bar*) and in the presence (Fig. 1 *M*, *red bar*) of 5 mM serotonin are 0.48 ± 0.02 and 0.63 ± 0.01, respectively. The average GP value increases by 31% ± 5% in the presence of 5 mM serotonin, indicating that the PPC111 bilayer becomes more ordered in the presence of serotonin.

Steady-state anisotropy of DPH and TMA-DPH dyes

We have performed the steady-state anisotropy measurement of PPC111 vesicles doped with DPH and TMA-DPH dyes with increasing concentrations of serotonin to measure the rotational dynamics of probes in the vesicles, which in turn provides the information of lipid packing or membrane order. DPH is located at an average distance of approximately 7.8 Å from the center of the bilayer, whereas its trimethylammonium derivative (TMA-DPH) partitions at the interfacial region of the membrane (10.9 Å from the center of the bilayer) because of its charge. Therefore, fluorescence anisotropy of DPH and TMA-DPH provide information of membrane order at two different regions of the membrane (50). We found that rotational anisotropy increases in the presence of serotonin in both dyes (Fig. 1 *N* and *O*). The average anisotropy of DPH and TMA-DPH increases by 38% ± 3% and 5% ± 1% at 0.5 mM serotonin, respectively. This suggests that the rotation of lipids slowed down in the presence of serotonin in the PPC111 vesicles, indicating that the membrane becomes more ordered in the presence of serotonin.

Raman spectroscopy measurements

The Raman spectra of PPC111 SLB in the absence and presence of 20 mM serotonin are measured at ∼ 2850, ∼2885, and ∼2930 cm^{-1}. The representative normalized Raman spectra for fresh PPC111 SLB (black) and serotonin-containing SLB (light brown) are shown in Fig. 1 *P*. For the PPC111 membrane, serotonin showed an average increase of 11% ± 2% in the I_{2885}/I_{2850} ratio, indicating an increase of the CH_2 conformational order (Fig. 1 *Q*, *left*). However, the I_{2850}/I_{2930} ratio decreases by 45% ± 3% (Fig. 1 *Q*, *right*), suggesting that the local order near the terminal CH_3 decreases upon incubation with serotonin.

Solid-state NMR

In a previous study (25), we had also measured the ^{2}H NMR order parameter of the PPC111 vesicles in the absence and the presence of 10 mol % serotonin (relative to the lipid) using ^{2}H solid-state NMR. The NMR measurements have shown that the order parameter of the PPC111 bilayer along the lipid acyl chains for deuterated POPC and POPG decreases in the presence of serotonin both at 25°C and 37°C (Fig. 1 *R*, reproduced from Dey et al. (25)). This

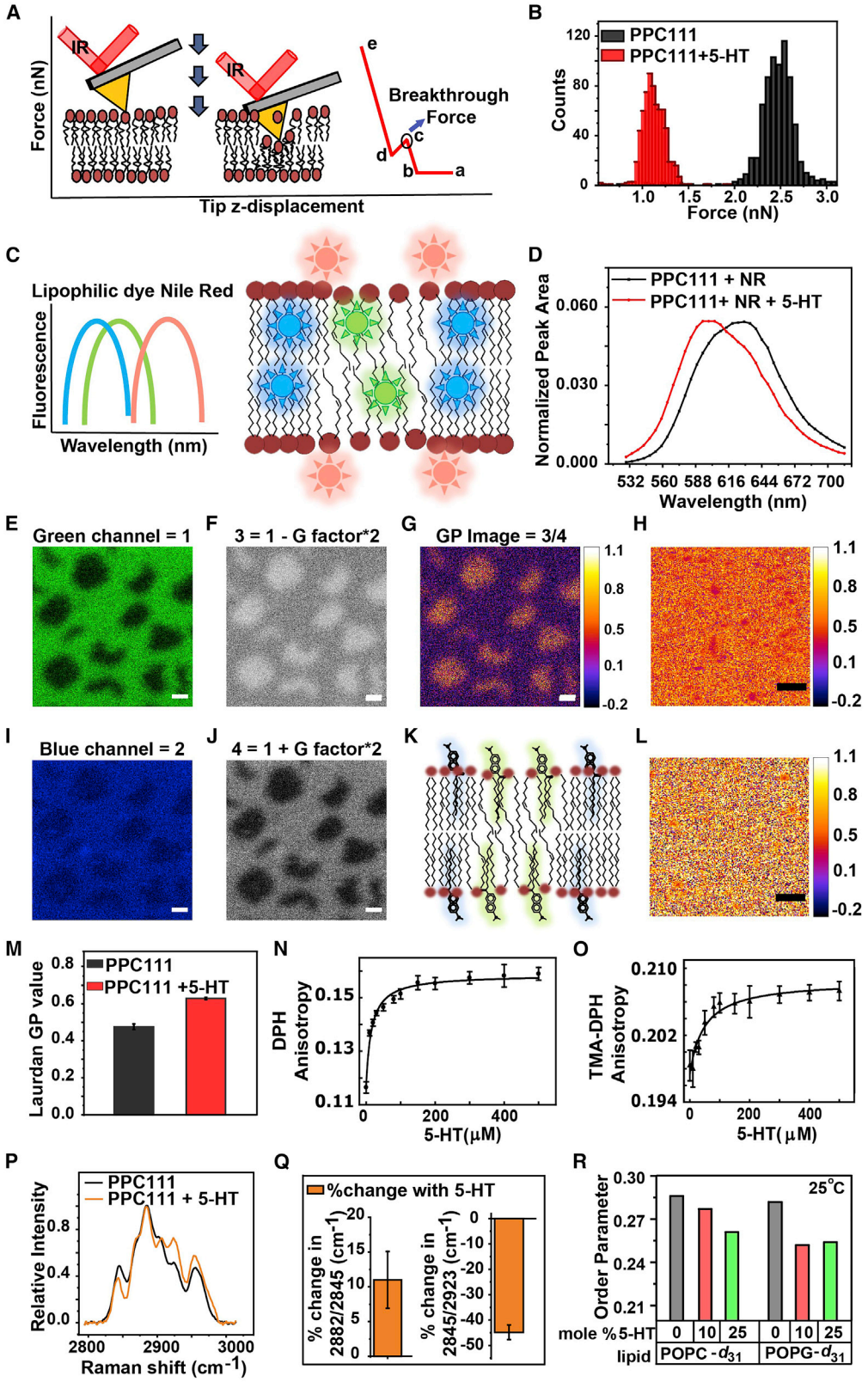

FIGURE 1 Effect of serotonin on the mechanical properties of PPC111 bilayer probed by different biophysical techniques. (*A*) Schematic of the AFM force indentation studies. (*B*) A representative histogram of breakthrough forces on the PPC111 bilayer in the absence (*black*) and presence (*red*) of 5 mM serotonin (reproduced from Dey et al. (25)). (*C*) Schematic of the fluorescence spectral properties of Nile Red in different membrane environments. (*D*) Fluorescence spectra of membrane-bound Nile Red dye in PPC111 bilayer in the absence (*black*) and presence (*red*) of 5 mM serotonin (average of $N = 3$

(legend continued on next page)

suggests that the PPC111 membrane becomes more disordered upon adding serotonin.

Serotonin induced perturbations of POPG and DEC221 membranes

The investigations of the PPC111 membrane suggested that different techniques and probes used to measure the membrane order frequently do not provide results that correlate with each other. To investigate if this is peculiar to the type of membrane we have used, we probed two other membrane compositions, POPG and DEC221. Among these, DEC221 is a biphasic bilayer, and the ordered (L_o) and disordered (L_d) domains can be clearly identified in AFM imaging. We measured several other parameters also to test their correlation with F_X. The effect of 5 mM serotonin on the F_X of each of these bilayers could be measured with AFM. The detailed results for POPG and for the L_o and L_d domains of DEC221 are given in the supporting material (sections S2.1 and S2.2). In summary, for POPG membranes, the average F_X increases by 368% ± 158%. Nile Red spectra shift to shorter wavelengths with G/R value increasing from 0.34 ± 0.04 to 0.66 ± 0.05, representing a 94% ± 22% increase and implying a substantial increase of membrane order. However, there is no change observed in the NMR order parameter in the presence of serotonin (supporting material, section S2.1; Fig. S1).

For the biphasic DEC221 membrane, the average Fx decreases by 52.0% ± 8.3% and 32.0% ± 10.3% in the L_o and L_d phases, respectively. Nile Red spectra shift to a lower wavelength, and the G/R value increases from 0.78 ± 0.01 to 0.85 ± 0.05 in the presence of serotonin for the L_o phase (average G/R value increases by 9% ± 6%). For the L_d phase, the G/R value increases from 0.52 ± 0.01 to 0.59 ± 0.02 (average G/R value increases by 13% ± 4%), indicating minimal changes. However, the Laurdan GP value increases from −0.16 ± 0.01 to −0.06 ± 0.01 in the L_d phase and from 0.30 ± 0.05 to 0.42 ± 0.06 in the L_o phase. Thus, the average GP value for Laurdan increases substantially by 40% ± 27% and 63% ± 10% in the L_o and L_d phases, respectively. The average translational diffusion coefficient D_T, as measured by z-scan FCS, decreases from 5.4 ± 0.5 to 1.6 ± 0.1 $\mu m^2 s^{-1}$, indicating an average decrease in D_T by 70% ± 11% in the presence of 5 mM serotonin (supporting material, section S2.2; Fig. S2). In our previous studies, we have measured the NMR order parameter for a biphasic membrane system PEC221 (except DOPC in DEC221, this membrane contained POPC, which could be chain deuterated) in the absence and the presence of serotonin. The NMR order parameter decreased in the disordered phase and increased in the ordered phase in the presence of 9 mol % serotonin (46).

In order to compare the different measurements (which have different units), we have plotted a histogram of changes measured in units of standard deviation for each type of measurement (Fig. 2). In relative terms, this shows how significant the changes are. Fig. 2 *A* represents measurements made on PPC111, while Fig. 2 *B–D* represent measurements on POPG, DEC221 (L_d), and DEC 221 (L_o), respectively.

DISCUSSION

The term order of a membrane refers to a unifying concept that is assumed to characterize a host of properties of the bilayer. For example, a decrease in membrane order is expected to make it easier to produce a disruption in the membrane, rendering the acyl chains of the lipids more dynamic and the hydrophobic interior partially polar and consequently allowing more efficient diffusion of a probe into the membrane. Each of these properties can be measured with a set of different techniques. The change in membrane order upon the addition of a perturbant is expected to reflect in all these measurements, at least qualitatively. A few studies have validated this assumption, but they have compared only a few techniques (24,26,41,42). Here, we have employed a large variety of techniques (9 in total) to measure the change in the membrane order by small molecules known to modulate the membrane properties.

We have studied the effect of serotonin, a small lipophilic molecule known to modulate the membrane properties (25,46–48), on the model membrane mixture PPC111. Serotonin is an archetypal monoamine neurotransmitter that is known to have long-term neuromodulatory effects compared with typical neurotransmitters (51–53). A modulation of the membrane properties can be a putative pathway of its action (25). It is also packed at 100s of mM concentration in the vesicles (54) and therefore can have a significant

measurements). (*E–G*, *I*, and *J*) Calculation of the generalized polarization (GP) of Laurdan in supported phase-separated model membrane DEC221. (*E*) and (*I*) are images recorded in the green and blue regions. (*F*) and (*J*) are the images obtained with the indicated formula to generate images 3 and 4. (*G*) The GP image. (*K*) Schematic of the fluorescence spectral properties of Laurdan in ordered and disordered membrane environments. (*H*) Representative GP image of PPC111 SLB. (*L*) Representative GP image of PPC111 SLB in the presence of 5 mM serotonin. Scale bar: 10 μm. (*M*) GP value of Laurdan dye in the PPC111 bilayer in the absence (*black*) and presence (*red*) of 5 mM serotonin (average of $N = 3$ measurements). (*N* and *O*) Changes in the rotational anisotropy of DPH and TMA-DPH dyes in the PPC111 SLB with increasing concentrations of serotonin probed by steady-state anisotropy experiments. (*P*) A representative Raman spectrum (normalized at 2885 cm^{-1}) of the PPC111 SLB in the absence (*black*) and presence (*light brown*) of 20 mM serotonin. (*Q*) Relative change in the mean value of I_{2882}/I_{2845} and I_{2845}/I_{2923} of PPC111 bilayer in the presence of 20 mM serotonin (average of $N = 5$ measurements). (*R*) ^2H NMR order parameter along the deuterated lipid chains for POPC-d_{31} and POPG-d_{31} in the absence and presence of 10 mol % serotonin at 25°C (reproduced from Dey et al. (25)). Error bar represents mean ± SE.

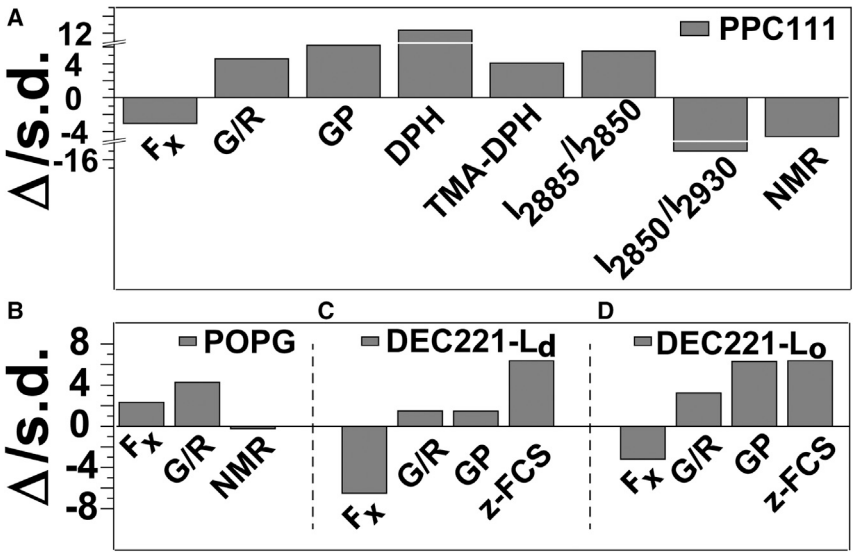

FIGURE 2 A comparison of measurements of serotonin-induced changes between different techniques. The changes are represented in units of the standard deviation of the measurements. Δ, change upon serotonin addition (after – before); s.d., standard deviation. (*A–D*) The figures represent measurements obtained from different techniques on PPC111 (*A*), POPG (*B*), disordered phase L_d of DEC221 (*C*), and ordered phase L_o of DEC221 (*D*). Positive change means order increases upon serotonin incubation.

effect on the membrane. So, its interaction with the lipid membrane assumes strong biological significance. We employed AFM force indentation (F_X), Nile Red fluorescence spectral studies (G/R), NMR order parameter (NMR), Laurdan GP (GP), DPH and TMA-DPH steady-state anisotropy, and ratiometric Raman spectroscopy of lipid modes (I_{2885}/I_{2850} and I_{2850}/I_{2930}). We note that the serotonin/lipid molar ratio is not the same for all the techniques employed. For a PPC111 vesicle at 5 mM serotonin, the partition coefficient is 1500, indicating that there is 11% serotonin/lipid molar ratio in the membrane (25). We add a note of caution that this is only an estimate, and this number can vary for a supported lipid bilayer. However, it shows that the molar ratios are of the same order of magnitude in the different experiments. In addition, we also note that the concentration of the perturbant is expected to govern the extent of change in the membrane order but not the direction of change. So, our main conclusion remains robust with respect to differences in the exact concentration of serotonin in different experiments. AFM force indentation, NMR order parameter, and Raman I_{2850}/I_{2930} ratio measurements suggest that the PPC111 membrane becomes more disordered upon incubation with serotonin (Fig. 2 *A*). However, Nile Red spectral shift in terms of the G/R ratio, Laurdan GP value, DPH and TMA-DPH anisotropy, and Raman I_{2885}/I_{2850} ratio measurements show that the PPC111 membrane becomes more ordered in the presence of serotonin.

All these results strongly suggest that different techniques may measure somewhat different properties of the membrane. However, we could still find the correlation between a subgroup of techniques, such as AFM and NMR. This raises the possibility that a specific group of techniques may always correlate with each other and thus could be placed under a common category.

This possibility is investigated by probing a different membrane composition, namely POPG. F_X and G/R measurements suggest that serotonin makes the POPG membrane more ordered (Fig. 2 *B*). However, NMR shows that serotonin does not alter the order of the POPG membrane. This is opposite to what we have observed in the case of the PPC111 membrane and shows that a given pair of techniques do not always correlate with one another.

We have also studied the effect of serotonin on the order of biphasic model membrane DEC221, which forms coexisting ordered and disordered phases. Each membrane phase has distinct membrane order, thus how different probes respond to these phases can be studied simultaneously on the same membrane. We found that different probes could differentiate between the mechanical properties of the two phases. However, F_X is anticorrelated with G/R, GP, and z-FCS measurements in both the phases (Fig. 2 *C* and *D*), so different techniques do not even agree between two neighboring phases on the same membrane.

Thus, we found a lack of universal correlation between different types of techniques, with no consistent rule predicting whether two types of techniques would correlate with each other. This lack of correlation is also observed for different membrane compositions, suggesting that our finding is not limited to a particular membrane mixture. Our study also highlights that the correlation found between a few techniques in the previous studies is probably a coincidence. For instance, there are studies that have shown the correlation of Laurdan GP with NMR order parameters (42) and AFM F_X measurements (26). But in our study on the PPC111 bilayer, both the techniques are anticorrelated with Laurdan GP measurements. While the reason for this is not clear right now, it is obvious that the assumption that all probes report a perturbation of the bilayer in a single consistent way is not correct. Different techniques mainly measure the membrane properties depending on the localization of the probes and on the temporal and spatial scales of the techniques. Thus, it is important to understand how

each of these parameters are related to a specific property of the membrane instead of implying that any of it is an average measurement of membrane order. It is worth noting that, as of now, our findings hold for the perturbant serotonin. We do not have proof that this discrepancy can be generalized beyond serotonin. However, we expect that the effect is more general. Any small molecule engaged in headgroup interactions similar to serotonin may lead to this response. We are currently carrying out measurements involving other neurotransmitters as well as other membrane-active molecules.

Finally, the issue of probe-related versus probe-free measurements of membrane order remains. We note that the direction of change measured by different fluorescence spectroscopy-based techniques are generally correlated, though their amplitudes are frequently not. For example, the Laurdan GP value shows only a small increase of membrane order in the disordered domain of DEC221 but a robust increase in the ordered domains (Fig. 2 *C* and *D*). On the other hand, z-FCS shows increase of similar magnitudes in both the phases. Although heavily debated ever since such measurements were introduced, it is agreed that bulky fluorescence probes may represent a local perturbation of lipid packing, while AFM and NMR techniques directly measure membrane order (neglecting isotope effects in NMR measurements). Clearly, molecular parameters such as probe amplitude, correlation time of motion, etc., are not comparable between the methods. Molecular order is not "static" but does depend on the time window over which motions are sampled. Lipid membranes are subject to complex dynamic landscapes and holistic concepts are required to fully describe membrane order and elasticity, typically involving the combination of several experimental and computational techniques (55). For instance, molecular dynamics simulations, Monte Carlo simulations, or theoretical modeling can be used to mimic the experimental response of a particular probe in the membranes. Such studies will improve our understanding of what exactly these probes are measuring in the membrane.

CONCLUSIONS

The lipid bilayer is characterized by the heterogeneous distribution of various lipid headgroups, acyl tails, and surface, interfacial, and percolated water in the acyl chain region. Individual as well as collective behavior of these different components generate lateral and *trans*-bilayer heterogeneity in terms of polarity, lateral and rotational diffusion of lipids, viscosity, and hydration of the membrane. All the techniques that are used to determine membrane order do not measure the same property of the membrane. For example, AFM F_X measurements directly determine the mechanical stability of the lipid bilayer, whereas fluorescence-based measurements are mostly dependent on the rotational flexibility and polarity of the lipidic microenvironment at the place where the probe is located. Therefore, it is perhaps not surprising that the membrane order parameters obtained from different techniques are not correlated. In conclusion, a generalized notion of membrane order is best avoided, and one must be cautious in drawing biological inferences from it. A correlation of relevant functions and membrane properties must first be established before drawing any inference from a particular measurement.

SUPPORTING MATERIAL

Supporting material can be found online at https://doi.org/10.1016/j.bpj.2022.08.029.

AUTHOR CONTRIBUTIONS

D.H. and S.M. designed experiments and conceptualized the study. A.G., M.K., D.S.R., O.E., and H.C. performed experiments and analyzed data. S.M. wrote article with input and contributions from all coauthors.

ACKNOWLEDGMENTS

We dedicate this study to Dr. Klaus Gawrisch, our mentor, friend, and most highly appreciated colleague. Membrane order is a topic that has always been inspired and much benefited from Klaus's seminal contributions. The scientific advice, encouragements, and critical and very constructive support throughout the last 30 years are highlighting his great contributions to membrane biophysics. D.H. thanks Klaus very personally for his friendship, support, help, and career advice; without you, Klaus, I would not be where I am.

This work was supported by the department of Atomic Energy, Goverment of India, provided under project no RTI4003. O.E. acknowledges support by the Magnus Ehrnrooth foundation, and Ruth and Nils-Erik Stenbäck's Foundation.

DECLARATION OF INTERESTS

The authors declare no competing interests.

REFERENCES

1. Bozelli, J. C., and R. M. Epand. 2020. Determinants of lipids acyl chain specificity: a tale of two enzymes. *Biophys. Chem.* 265:106431. https://doi.org/10.1016/J.BPC.2020.106431.
2. Cheng, X., and J. C. Smith. 2019. Biological membrane organization and cellular signaling. *Chem. Rev.* 119:5849–5880. https://doi.org/10.1021/acs.chemrev.8b00439.
3. Muller, M. P., T. Jiang, …, E. Tajkhorshid. 2019. Characterization of lipid-protein interactions and lipid-mediated modulation of membrane protein function through molecular simulation. *Chem. Rev.* 119:6086–6161. https://doi.org/10.1021/acs.chemrev.8b00608.
4. Faustino, I., H. Abdizadeh, …, S. J. Marrink. 2020. Membrane mediated toppling mechanism of the folate energy coupling factor transporter. *Nat. Commun.* 11:1763–1769. https://doi.org/10.1038/s41467-020-15554-9.
5. Bozelli, J. C., S. S. Aulakh, and R. M. Epand. 2021. Membrane shape as determinant of protein properties. *Biophys. Chem.* 273:106587. https://doi.org/10.1016/J.BPC.2021.106587.

6. Oseid, D. E., L. Song, …, A. S. Robinson. 2020. Nuclear translocation of the unliganded glucocorticoid receptor is influenced by membrane fluidity, but not A2AR agonism. *Steroids.* 160:108641. https://doi.org/10.1016/j.steroids.2020.108641.
7. Giacomello, M., A. Pyakurel, …, L. Scorrano. 2020. The cell biology of mitochondrial membrane dynamics. *Nat. Rev. Mol. Cell Biol.* 21:204–224. https://doi.org/10.1038/s41580-020-0210-7.
8. Zielińska, A., A. Savietto, …, D. J. Scheffers. 2020. Flotillin-mediated membrane fluidity controls peptidoglycan synthesis and MreB movement. *Elife.* 9. . e57179–21. https://doi.org/10.7554/ELIFE.57179.
9. Sastre, D. E., L. G. M. Basso, …, M. E. Guerin. 2020. Membrane fluidity adjusts the insertion of the transacylase PlsX to regulate phospholipid biosynthesis in gram-positive bacteria. *J. Biol. Chem.* 295:2136–2147. https://doi.org/10.1074/jbc.RA119.011122.
10. Lee, S. M., S. H. Lee, …, K. S. Kwon. 2020. FABP3-mediated membrane lipid saturation alters fluidity and induces ER stress in skeletal muscle with aging. *Nat. Commun.* 11:5661–5715. https://doi.org/10.1038/s41467-020-19501-6.
11. Gastaldo, I. P., H. V. Rheinstädter, and M. C. Rheinstädter. 2020. Perspective on the role of the physical properties of membranes in neurodegenerative and infectious diseases. *Appl. Phys. Lett.* 117:040501. https://doi.org/10.1063/5.0018709.
12. Bianchetti, G., L. Viti, …, G. Maulucci. 2021. Erythrocyte membrane fluidity as a marker of diabetic retinopathy in type 1 diabetes mellitus. *Eur. J. Clin. Invest.* 51. . e13455–6. https://doi.org/10.1111/eci.13455.
13. Dadhich, R., M. Mishra, …, S. Kapoor. 2020. A virulence-associated glycolipid with distinct conformational attributes: impact on lateral organization of host plasma membrane, autophagy, and signaling. *ACS Chem. Biol.* 15:740–750. https://doi.org/10.1021/acschembio.9b00991.
14. Bompard, J., A. Rosso, …, O. Maniti. 2020. Membrane fluidity as a new means to selectively target cancer cells with fusogenic lipid carriers. *Langmuir.* 36:5134–5144. https://doi.org/10.1021/acs.langmuir.0c00262.
15. Kucherak, O. A., S. Oncul, …, A. S. Klymchenko. 2010. Switchable Nile Red-based probe for cholesterol and lipid order at the outer leaflet of biomembranes. *J. Am. Chem. Soc.* 132:4907–4916. https://doi.org/10.1021/ja100351w.
16. Moon, S., R. Yan, …, K. Xu. 2017. Spectrally resolved, functional super-resolution microscopy reveals nanoscale compositional heterogeneity in live-cell membranes. *J. Am. Chem. Soc.* 139:10944–10947. https://doi.org/10.1021/jacs.7b03846.
17. Sanchez, S. A., M. A. Tricerri, and E. Gratton. 2012. Laurdan generalized polarization fluctuations measures membrane packing micro-heterogeneity in vivo. *Proc. Natl. Acad. Sci. USA.* 109:7314–7319. https://doi.org/10.1073/pnas.1118288109.
18. Kaiser, H. J., D. Lingwood, …, K. Simons. 2009. Order of lipid phases in model and plasma membranes. *Proc. Natl. Acad. Sci. USA.* 106:16645–16650. https://doi.org/10.1073/pnas.0908987106.
19. Halder, A., B. Saha, …, S. Karmakar. 2018. Lipid chain saturation and the cholesterol in the phospholipid membrane affect the spectroscopic Properties of lipophilic dye Nile Red. *Spectrochim. Acta Mol. Biomol. Spectrosc.* 191:104–110. https://doi.org/10.1016/j.saa.2017.10.002.
20. Parasassi, T., G. de Stasio, …, E. Gratton. 1991. Quantitation of lipid phases in phospholipid vesicles by the generalized polarization of Laurdan fluorescence. *Biophys. J.* 60:179–189. https://doi.org/10.1016/S0006-3495(91)82041-0.
21. Zhang, Y. L., J. A. Frangos, and M. Chachisvilis. 2006. Laurdan fluorescence senses mechanical strain in the lipid bilayer membrane. *Biochem. Biophys. Res. Commun.* 347:838–841. https://doi.org/10.1016/j.bbrc.2006.06.152.
22. Filipe, H. A. L., M. J. Moreno, and L. M. S. Loura. 2020. The secret lives of fluorescent membrane probes as revealed by molecular dynamics simulations. *Molecules.* 25:E3424–E3443. https://doi.org/10.3390/molecules25153424.
23. Sezgin, E., T. Sadowski, and K. Simons. 2014. Measuring lipid packing of model and cellular membranes with environment sensitive probes. *Langmuir.* 30:8160–8166. https://doi.org/10.1021/la501226v.
24. Moulton, E. R., K. J. Hirsche, …, J. D. Bell. 2018. Examining the effects of cholesterol on model membranes at high temperatures: Laurdan and Patman see it differently. *Biochim. Biophys. Acta Biomembr.* 1860:1571–1579. https://doi.org/10.1016/j.bbamem.2018.05.013.
25. Dey, S., D. Surendran, …, S. Maiti. 2021. Altered membrane mechanics provides a receptor-independent pathway for serotonin action. *Chemistry.* 27:7533–7541. https://doi.org/10.1002/chem.202100328.
26. Monasterio, B. G., N. Jiménez-Rojo, …, A. Alonso. 2020. Patches and blebs: a comparative study of the composition and biophysical properties of two plasma membrane preparations from CHO cells. *Int. J. Mol. Sci.* 21:26433–E2711. https://doi.org/10.3390/ijms21072643.
27. Sengupta, P., J. Balaji, and S. Maiti. 2002. Measuring diffusion in cell membranes by fluorescence correlation spectroscopy. *Methods.* 27:374–387. https://doi.org/10.1016/S1046-2023(02)00096-8.
28. Steinberger, T., R. Macháň, and M. Hof. 2014. Z-scan fluorescence correlation spectroscopy as a Ttool for diffusion measurements in planar lipid membranes. *Methods Mol. Biol.* 1076:617–634. https://doi.org/10.1007/978-1-62703-649-8_28.
29. Wallach, D. F., S. P. Verma, and J. Fookson. 1979. Application of laser Raman and infrared spectroscopy to the analysis of membrane structure. *Biochim. Biophys. Acta Rev. Biomembr.* 559:153–208. https://doi.org/10.1016/0304-4157(79)90001-7.
30. Gaber, B. P., and W. L. Peticolas. 1977. On the quantitative interpretation of biomembrane structure by Raman spectroscopy. *Biochim. Biophys. Acta.* 465:260–274. https://doi.org/10.1016/0005-2736(77)90078-5.
31. Davis, J. H. 1983. The description of membrane lipid conformation, drder and dynamics by 2H-NMR. *Biochim. Biophys. Acta.* 737:117–171. https://doi.org/10.1016/0304-4157(83)90015-1.
32. Molugu, T. R., S. Lee, …, M. F. Brown. 2017. Concepts and methods of solid-state NMR spectroscopy applied to biomembranes. *Chem. Rev.* 117:12087–12132. https://doi.org/10.1021/acs.chemrev.6b00619.
33. Huster, D., K. Arnold, and K. Gawrisch. 1998. Influence of docosahexaenoic acid and cholesterol on lateral lipid organization in phospholipid mixtures. *Biochemistry.* 37:17299–17308. https://doi.org/10.1021/bi980078g.
34. Leftin, A., T. R. Molugu, C. Job, K. Beyer, and M. F. Brown. 2014. Area per lipid and cholesterol interactions in membranes from separated local-field 13C NMR spectroscopy. *Biophys. J.* 107:2274–2286. https://doi.org/10.1016/J.BPJ.2014.07.044.
35. Ferreira, T. M., F. Coreta-Gomes, …, D. Topgaard. 2013. Cholesterol and POPC segmental order parameters in lipid membranes: solid state 1H–13C NMR and MD simulation studies. *Phys. Chem. Chem. Phys.* 15:1976–1989. https://doi.org/10.1039/C2CP42738A.
36. Hassan-Zadeh, E., F. Hussain, and J. Huang. 2017. Gramicidin peptides alter global lipid compositions and bilayer thicknesses of coexisting liquid-ordered and liquid-disordered membrane domains. *Langmuir.* 33:3324–3332. https://doi.org/10.1021/acs.langmuir.6b03688.
37. Gaus, K., S. Le Lay, …, M. A. Schwartz. 2006. Integrin-mediated adhesion regulates membrane order. *J. Cell Biol.* 174:725–734. https://doi.org/10.1083/jcb.200603034.
38. Zorilă, B., G. Necula, …, M. Bacalum. 2020. Melittin induces local order changes in artificial and biological membranes as revealed by spectral analysis of Laurdan fluorescence. *Toxins.* 12:1210705. https://doi.org/10.3390/toxins12110705.
39. Bernardes, N., A. R. Garizo, …, A. M. Fialho. 2018. Azurin interaction with the lipid raft components ganglioside GM-1 and caveolin-1 increases membrane fluidity and sensitivity to anti-cancer drugs. *Cell Cycle.* 17:1649–1666. https://doi.org/10.1080/15384101.2018.1489178.
40. Lorizate, M., B. Brügger, …, H. G. Kräusslich. 2009. Probing HIV-1 membrane liquid order by Laurdan staining reveals producer cell-dependent differences. *J. Biol. Chem.* 284:22238–22247. https://doi.org/10.1074/jbc.M109.029256.
41. Steinkühler, J., E. Sezgin, …, R. Dimova. 2019. Mechanical properties of plasma membrane vesicles correlate with lipid order, viscosity and cell density. *Commun. Biol.* 2:337–338. https://doi.org/10.1038/s42003-019-0583-3.

42. Leung, S. S. W., J. Brewer, …, J. L. Thewalt. 2019. Measuring molecular order for lipid membrane phase studies: linear relationship between Laurdan generalized polarization and deuterium NMR order parameter. *Biochim. Biophys. Acta Biomembr.* 1861:183053. https://doi.org/10.1016/j.bbamem.2019.183053.

43. Postila, P. A., and T. Róg. 2020. A perspective: active role of lipids in neurotransmitter dynamics. *Mol. Neurobiol.* 57:910–925. https://doi.org/10.1007/s12035-019-01775-7.

44. Peters, G. H., C. Wang, …, P. Westh. 2013. Binding of serotonin to lipid membranes. *J. Am. Chem. Soc.* 135:2164–2171. https://doi.org/10.1021/ja306681d.

45. Josey, B. P., F. Heinrich, …, M. Lösche. 2020. Association of model neurotransmitters with lipid bilayer membranes. *Biophys. J.* 118:1044–1057. https://doi.org/10.1016/j.bpj.2020.01.016.

46. Engberg, O., A. Bochicchio, …, D. Huster. 2020. Serotonin alters the phase equilibrium of a ternary mixture of phospholipids and cholesterol. *Front. Physiol.* 11:578868–578914. https://doi.org/10.3389/fphys.2020.578868.

47. Bochicchio, A., A. F. Brandner, …, R. A. Böckmann. 2020. Spontaneous membrane nanodomain formation in the absence or presence of the neurotransmitter serotonin. *Front. Cell Dev. Biol.* 8:601145–601217. https://doi.org/10.3389/fcell.2020.601145.

48. Musabirova, G., O. Engberg, …, D. Huster. 2022. Serotonergic drugs modulate the phase behavior of complex lipid bilayers. *Biochimie*, . In press. https://doi.org/10.1016/j.biochi.2022.04.006.

49. Leonenko, Z. V., A. Carnini, and D. T. Cramb. 2000. Supported planar bilayer formation by vesicle fusion: the interaction of phospholipid vesicles with surfaces and the effect of gramicidin on bilayer properties using atomic force microscopy. *Biochim. Biophys. Acta.* 1509:131–147. https://doi.org/10.1016/S0005-2736(00)00288-1.

50. Kaiser, R. D., and E. London. 1998. Location of diphenylhexatriene (DPH) and its derivatives within membranes: comparison of different fluorescence quenching analyses of membrane depth. *Biochemistry.* 37:8180–8190. https://doi.org/10.1021/bi980064a.

51. Coray, R., and B. B. Quednow. 2022. The role of serotonin in declarative memory: a systematic review of animal and human research. *Neurosci. Biobehav. Rev.* 139:104729. https://doi.org/10.1016/j.neubiorev.2022.104729.

52. Murano, M., F. Saitow, and H. Suzuki. 2011. Modulatory effects of serotonin on glutamatergic synaptic transmission and long-term depression in the deep cerebellar nuclei. *Neuroscience.* 172:118–128. https://doi.org/10.1016/j.neuroscience.2010.10.037.

53. Hirono, M., F. Karube, and Y. Yanagawa. 2021. Modulatory effects of monoamines and perineuronal nets on output of cerebellar purkinje cells. *Front. Neural Circ.* 15:661899. https://doi.org/10.3389/fncir.2021.661899.

54. Balaji, J., R. Desai, …, S. Maiti. 2005. Quantitative measurement of serotonin synthesis and sequestration in individual live neuronal cells. *J. Neurochem.* 95:1217–1226. https://doi.org/10.1111/j.1471-4159.2005.03489.x.

55. Smith, A. A., A. Vogel, …, D. Huster. 2022. A method to construct the dynamic landscape of a bio-membrane with experiment and simulation. *Nat. Commun.* 13:108. https://doi.org/10.1038/s41467-021-27417-y.